Theor Appl Genet (2004) 109: 899–910
DOI 10.1007/s00122-004-1717-6

ORIGINAL PAPER

Mingliang Xu · Xiangqian Li · Schuyler S. Korban

DNA-methylation alterations and exchanges during in vitro cellular differentiation in rose (*Rosa hybrida* L.)

Received: 28 October 2003 / Accepted: 27 April 2004 / Published online: 19 June 2004
© Springer-Verlag 2004

Abstract DNA-methylation profiles of leaf tissues of *Rosa hybrida* cv. Carefree Beauty collected from in vivo-grown greenhouse plants, in vitro-grown proliferating shoots at different passages, regenerants of embryogenic callus, regenerants of organogenic callus, as well as calli from undifferentiated callus (UC), embryogenic callus, and organogenic callus were investigated using an amplified fragment-length polymorphism (AFLP)-based detection technique. Three types of AFLP bands were recovered. Type I bands were observed with both isoschizomers *Msp* and *Hpa*II, while type II and type III bands were observed only with *Msp*I and *Hpa*II, respectively. Sequence analysis of the three types of AFLP bands revealed that a nonmethylated *Msp*I/*Hpa*II-recognition site 5′-CCGG-3′ resulted in a type I band, while an inner 5-methylcytosine generated most type II and type III bands. About 40% of inner and 20% of outer cytosines in 5′-CCGG-3′ sequences were fully methylated, and only a few hemimethylated outer cytosines were observed. Changes in types of AFLP bands among different tissues were frequently observed, including appearance and disappearance of type I, II, and III AFLP bands, as well as exchanges between either type I and type II or type I and type III AFLP bands. Methylation alterations of outer cytosines in 5′-CCGG-3′ sequences triggered appearance and disappearance of type I and II AFLP bands. Methylation changes of both outer and inner cytosines resulted in either removal or generation of type III AFLP bands. Methylation alteration of an inner cytosine was responsible for exchange between type I and type II, while hemimethylation of an outer cytosine accounted for exchange between type I and type III AFLP bands. During UC induction, a significant DNA-methylation alteration was detected in both inner and outer cytosines. Variations in methylation profiles significantly differed between somatic embryogenesis and in vitro organogenesis. Demethylation of outer cytosines occurred at a high frequency during somatic embryogenesis, and most altered AFLP bands in embryogenic callus were passed on to its regenerants. However, most methylation-altered AFLP bands during organogenesis were recovered in shoot regenerants derived via organogenic callus. Seven tissue-specific bands were isolated, cloned, and sequenced. Blast search revealed that two of these might be derived from functional genes.

Communicated by P. Langridge

Mingliang Xu and Xiangqian Li contributed equally to this paper

M. Xu · X. Li · S. S. Korban (✉)
Department of Natural Resources and Environmental Sciences, University of Illinois,
1201 W. Gregory, 310 ERML,
Urbana, IL 61801, USA
e-mail: korban@uiuc.edu
Fax: +1-217-333-8298

Present address:
M. Xu
China Agricultural University,
Beijing, PRC

Present address:
X. Li
Division of Biological Sciences, University of California–San Diego,
La Jolla, CA 92093, USA

Introduction

DNA methylation in both plant and mammalian systems has long been associated with changes in gene expression, chromatin structure alterations, activation of transposable elements, genomic imprinting, and carcinogenesis (Ferguson-Smith and Surani 2001; Finnegan 2001; Rossi et al. 1997; Stam et al. 1997; Wolffe and Matzke 1999). In eukaryotes and particularly in higher plants, 5-methylcytosine (5mC) is the predominant modified base (Ng and Bird 1999). Approximately 60–90% of all CpG sequences in a genome are methylated, while unmethylated CpG dinucleotides are mainly clustered in the CpG rich sequence—designated as a CpG island—of the promoter region of a gene (Ng and Bird 1999). In animal cells, 90–95% of methyl moieties are present in the dinucleotide

sequence 5mCpG (Stancheva et al. 2002). Finnegan et al. (2001) have reported that genome-wide demethylation has a pleiotropic effect on the regulation of developmental processes that take place in specific tissues or stages of development in plants. DNA methylation can inhibit transcription directly by blocking the binding of transcription factors by modifying their target sites. However, DNA methylation alone is often not sufficient to block transcription, but it is likely the form of chromatin on a methylated template that renders it transcriptionally inactive (Ng and Bird 1999). Moreover, proteins that bind methylcytosine, such as MeCp2, interact with a corepressor complex that includes histone deacetylase activity and results in transcriptional repression (Finnegan 2001). Alleviating this repression can be achieved by treatment with trichostatin A, an inhibitor of histone deacetylase, thus indicating that histone deacetylation is a crucial component of transcriptional repression by DNA methylation. This pathway—linking DNA methylation, histone deacetylation, and transcriptional repression—is conserved in mammals, but has not yet been confirmed in plants (Finnegan 2001). While methylation in mammalian genomes is generally restricted to CpG sequences, plant methylated cytosines have extensive asymmetric and CpXpG methylation, and genetic studies have revealed that a chromomethylase gene, *CMT3*, is a key determinant in CpXpG methylation (Bartee et al. 2001).

Somaclonal variation (phenotypic, karyotypic, biochemical, or genetic) observed in tissue culture has been documented (Duncan 1997; Kaeppler et al. 2000). Variation in DNA methylation induced by tissue culture has been suggested in part as the underlying molecular mechanism for somaclonal variation (Kaeppler et al. 2000). Somatic embryogenesis in carrot is one of the best-characterized cell differentiation systems in plants (Sung et al. 1984). Alterations in DNA methylation during somatic embryogenesis in carrot have been extensively investigated (LoSchiavo et al. 1989; Munksgaard et al. 1995). As concentrations of plant growth regulators (PGRs), such as 2,4-dichlorophenoxyacetic acid (2,4-D), 1-naphthaleneacetic acid, or indole 3-acetic acid increased in the medium, the amount of DNA methylation observed in carrot cells also increased (LoSchiavo et al. 1989). Moreover, the level of DNA methylation during early stages of cell differentiation is lower than that observed in later stages during somatic embryogenesis (Munksgaard et al. 1995).

The amplified fragment-length polymorphism (AFLP) technique has been modified to reveal DNA-methylation profiles in fungal, rice, *Arabidopsis*, apple, and *Pisum* genomes (Cervera et al. 2002; Li et al. 2002a; Knox and Ellis 2001; Reyna-López et al. 1997; Xiong et al. 1999; Xu et al. 2000). Recognition of tissue-specific AFLP bands has lead to the identification of functional genes that may alter their level of expression in certain tissues (Matthes et al. 2001).

Recently, an efficient method has been developed to induce both somatic embryogenesis and shoot organogenesis in *Rosa hybrida* cv. Carefree Beauty (Li et al. 2002b). It has been reported that reprogramming of somatic tissues

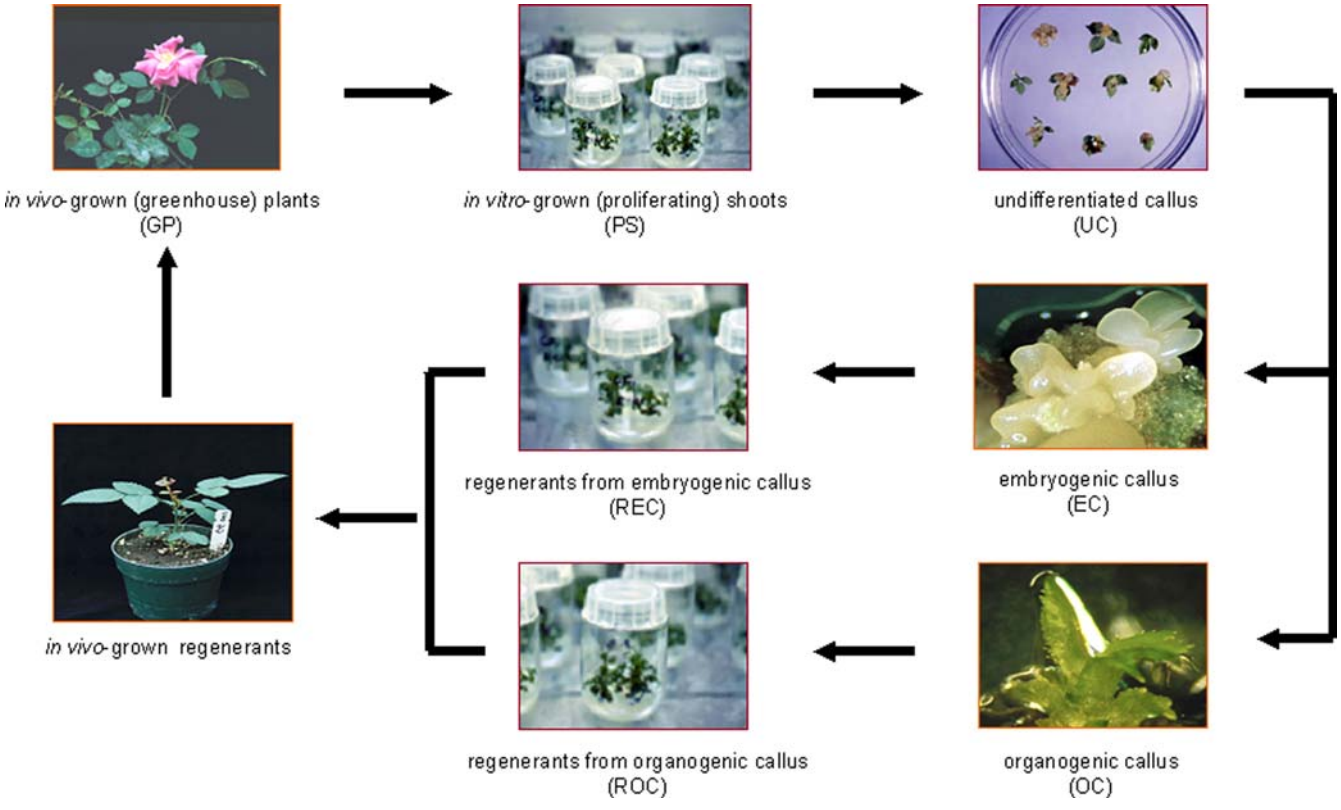

Fig. 1 Regeneration process of *Rosa hybrida* cv. Carefreee Beauty and tissues used for analysis of DNA methylation

for differentiation is accompanied by reprogramming of gene expression required for developmental switches (Hecht et al. 2001). Recently, Chakrabaty et al. (2003) have detected DNA-methylation changes during somatic embryogenesis of Siberian ginseng. However, there are no reports on monitoring DNA-methylation patterns undergoing distinct cellular differentiation pathways (organogenesis versus embryogenesis). It is likely that developmental pathways are affected by either misregulation of a key regulatory gene or through coordinated changes in expression, resulting from changes in methylation of many genes within the same pathway (Chakrabaty et al. 2003). Here, we provide a detailed analysis of DNA-methylation alterations during reprogramming events in somatic tissues of *Rosa* and investigate the nature of the relationship of these alterations with cellular-differentiation pathways undertaken by these somatic tissues.

Materials and methods

Plant material

All tissues used in this study are derived from *R. hybrida* cv. Carefree Beauty. The protocols of somatic embryogenesis and in vitro shoot organogenesis are briefly illustrated in Fig. 1.

Leaf tissues were harvested from in vivo-grown greenhouse plants (GP), in vitro-grown proliferating shoots (PS) at different passages (PS-1, PS-2, PS-9, and PS-15; numbers indicating months of subculture), regenerants of embryogenic callus (REC), and regenerants of organogenic callus (ROC). Calli were also collected from undifferentiated callus (UC), embryogenic callus (EC), and organogenic callus (OC). Undifferentiated callus (UC) was induced from leaf tissues of PS after 9-months of subculture (PS-9). All tissues were immediately frozen in liquid nitrogen, and stored in a −70°C ultrafreezer until needed.

DNA isolation and AFLP assay

Leaf tissue from individual shoots/plants and callus from pooled calli were used for DNA isolation. Genomic DNA (~0.25 μg) of both leaf tissues and calli was extracted using the Nucleon Phytopure Plant DNA Extraction Kit (Amersham Pharmacia Biotech), with some modifications as described by Xu et al. (2000). AFLP-based DNA-methylation detection was described by Xu et al. (2000). A total of 32 AFLP primer combinations, including eight *Eco*RI and four *Hpa*II–*Msp*I primers, were used in this study. To confirm accuracy of AFLP profiles, all reactions were repeated a second time, using fresh DNA samples. These DNA samples were extracted from the same corresponding frozen tissues previously collected.

Cluster analysis

AFLP bands on X-ray films were scored as 0 (missing band), 1 (type I), 2 (type II), and 3 (type III). Then, Jaccard's genetic coefficiency analysis was used to estimate similarity between each pair of tissues as described by Mumm and Dudley (1995). A hierarchical cluster analysis method was performed on a 10 × 10 genetic dissimilarity matrix (composed of coded AFLP bands), using the AVERAGE option of PROC CLUSTER of PC SAS (version 8.1) statistical analysis.

Tissue-specific and nonspecific AFLP bands, including types I, II, and III, were observed among ten different tissues used in the present study, thus generating various AFLP-banding patterns. The number of AFLP bands for each banding pattern was calculated, and banding patterns nos. 1, 2, and 3 corresponded to nonspecific AFLP bands type I, II, and III, respectively.

Cloning and validation of AFLP bands

Several AFLP bands, including nonspecific type I, II, and III AFLP bands and tissue-specific AFLP bands, were isolated from dried AFLP gels and cloned into a pBluescript KS vector according to our previously described protocol (Xu et al. 2001). Identification of cloned AFLP fragments also followed the procedure described previously (Xu et al. 2001). Each of the AFLP bands was then sequenced from both 5′ and 3′ ends.

Southern hybridization was used to further validate cloned AFLP bands (type I, II and III). A total of 10 μg genomic DNA from each tissue was digested separately with two sets of restriction enzymes, *Eco*RI/*Hpa*II and *Eco*RI/*Msp*I, and then subjected to electrophoresis using 1.0% agarose gel. Prehybridization, hybridization, and washing were performed as described by Sambrook et al. (1989). A 1-kb DNA ladder was used as a molecular-weight marker.

Blast search

Homology search was performed on the National Center for Biotechnology Information Blast server using both the nucleotide sequence and its deduced amino acid sequence for each tissue-specific AFLP band.

Table 1 A summary of type I, II, and III amplified fragment-length polymorphism (AFLP) bands for all ten tissues derived from *Rosa hybrida* cv. Carefree Beauty. AFLP-based DNA methylation was conducted using various tissues of *R. hybrida* cv. Carefree Beauty. DNA was isolated from various undifferentiated and differentiated tissues and subjected to AFLP analysis using a total of 32 AFLP primer combinations. AFLP bands were scored as type I, II, and III (as described in Materials and methods) for each tissue and summarized. The following tissues were analyzed: in vivo-greenhouse grown plants(*GP*), in vitro-grown shoots at various passages (*PS-1*, *PS-2*, *PS-9*, and *PS-15*), undifferentiated callus (*UC*), organogenic callus (*OC*), embryogenic callus (*EC*), regenerants from embryogenic callus (*REC*), and regenerants from organogenic callus (*ROC*)

Banding patterns	Leaf tissues							Callus		
	GP	PS-1	PS-2	PS-9	PS-15	ROC	REC	UC	OC	EC
Type I	811	772	776	766	770	770	830	797	793	866
Type II	513	507	511	507	514	501	530	486	487	515
Type III	140	139	139	137	141	148	139	160	152	133
Total	1,464	1,418	1,426	1,410	1,425	1,419	1,499	1,443	1,432	1,514

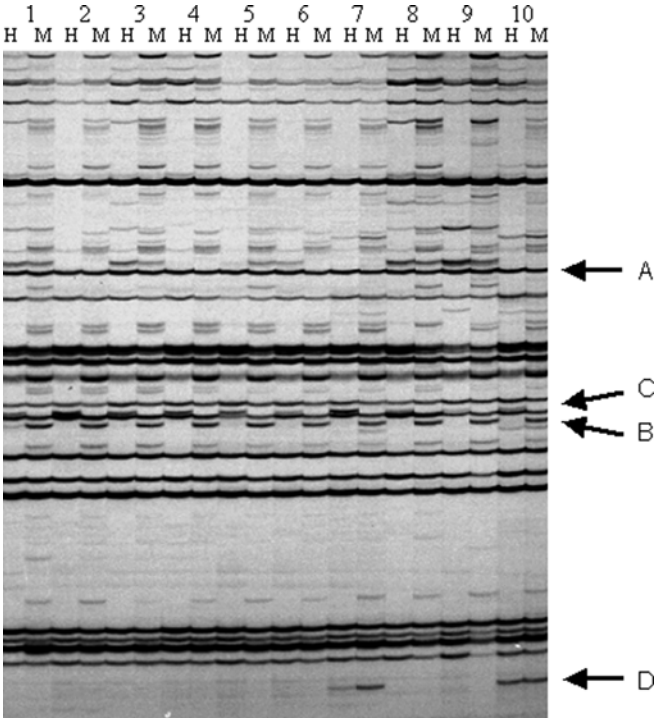

Fig. 2 DNA-methylation profiles using the primer combination of E-AC+HM-AG. *Lanes H* and *M* correspond to two sets of restriction enzyme combinations, *Eco*RI/*Hpa*II and *Eco*RI/*Msp*I, respectively. *Lane 1* In vivo-greenhouse-grown plants (*GP*); *lanes 2–5* in vitro-grown proliferating shoots at different passages, *PS-1*, *PS-2*, *PS-9*, and *PS-15*, respectively; *lane 6* regenerants from organogenic callus (*ROC*); *lane 7* regenerants from embryogenic callus (*REC*); *lane 8* undifferentiated callus (*UC*); *lane 9* organogenic callus (*OC,*); *lane 10* embryogenic callus (*EC*), respectively. *Arrows A*, *B*, *C*, and *D* indicate AFLP bands of type I (*A*), type II (*B*), type III (*C*), and tissue-specific AFLP band (*D*), respectively

Results

DNA-methylation profiles

For each of the rose tissues analyzed (Fig. 1), three types of AFLP bands were observed. Type I AFLP bands were present in both restriction enzyme combinations *Eco*RI/*Hpa*II and *Eco*RI/*Msp*I, while type II AFLP bands were present in *Eco*RI/*Msp*I but absent in *Eco*RI/*Hpa*II, and type III AFLP bands were present in *Eco*RI/*Hpa*II but absent in *Eco*RI/*Msp*I (Fig. 2). These were scored against 32 AFLP primer combinations and summarized in Table 1. Among all AFLP bands observed, the number of type I AFLP bands was greater than type II bands, and the number of type II bands was greater than type III bands. The average percentages were estimated to be 55.0 for type I, 35.3 for type II, and 9.7 for type III. Among the different tissues analyzed, a total of 1,514 and 1,499 AFLP bands were detected from EC and its REC, respectively, and these were the highest number of bands than in any of the other tissues (ranging from 1,410 in PS-9 to 1,464 in GP) (Table 1). These observed higher numbers of AFLP bands in EC and REC tissues are mainly attributed to an increase of type I AFLP bands.

As all ten types of tissues shared the same genomic background of *R. hybrida* cv. Carefree Beauty, variations in AFLP-banding patterns among the different tissues likely correspond to alterations in DNA methylation (Fig. 2). In order to reveal relationships among the different tissues, all AFLP-banding patterns were identified, and AFLP bands belonging to each of the banding patterns were scored (Table 2). Nonspecific type I, II, and III AFLP bands that were present in all tissues have been designated AFLP-banding patterns no. 1, 2, and 3, respectively. Tissue-specific AFLP bands were observed among all ten different tissues and resulted in additional 26 AFLP-banding patterns, each with at least three AFLP bands (Table 2). Various changes in banding types among the different tissues were observed, including appearance and disappearance of three types of AFLP bands, as well as exchanges between type I and either type II or type III bands. Following the cellular differentiation processes illustrated in Fig. 1, observed changes in AFLP bands in each of the steps during somatic embryogenesis and shoot organogenesis were calculated and listed in Table 3. When tissues from GPs were subjected to PS-9, 25 type I, 17 type II, and 14 type III AFLP bands disappeared (Table 3). Moreover, 20 type I bands changed into either type II or type III bands, and a few new type I, II, and III bands were observed (Table 3). PS at different passages (PS-1 to PS-15) and ROC exhibited high similarities in AFLP-banding patterns (Table 2). During induction of UC from a PS-9, numerous variations in DNA-methylation patterns were observed. These represented many changes in AFLP bands, including appearance of new bands, disappearance of old bands, and exchanges between bands (Table 3).

During the process of somatic embryogenesis, alterations in DNA methylation were found to be high from UC to EC, while those from EC to REC were found to be low. When UC tissues underwent differentiation to EC, a total of 34 type I, 29 type II, and 44 type III AFLP bands disappeared, while, 106 type I, 59 type II, and 16 type III AFLP bands were generated (Table 3). Most new AFLP bands (64 type I, 19 type II, and 6 type III) in EC tissue were then passed down to their REC (Table 2, nos. 17, 18, and 19). Moreover, 16 new type I bands in EC changed into type II in REC (Table 2, nos. 20). During the process of shoot organogenesis, many AFLP bands were modified as UC underwent organogenesis, and as OC underwent further development into ROC. This included disappearance and appearance of many type I, II, and III AFLP bands, as well as observed exchanges between either type I and type II or type I and type III bands (Table 3). Interestingly, the DNA-methylation status in ROC reverted back to the original profile observed in PS cultures, PS-9 (Table 2).

Based on similarities in DNA-methylation patterns, cluster analysis was conducted on ten different tissues (Fig. 3). ROC and in vitro-grown PS from four different passages (PS-1–PS-15) shared the highest similarities in DNA-methylation profiles and were clustered into one group. EC and its REC also shared high similarity in methylation profiles, and therefore were clustered into a

Table 2 Typical AFLP-banding patterns and their respective abundance in ten different tissues of rose (*R. hybrida* L). AFLP-banding patterns with at least three bands are listed. Different tissues from in vitro tissue culture of *R. hybrida* cv. Carefree Beauty have been subjected to AFLP-based DNA-methylation analysis

Banding pattern	GP	PS-1	PS-2	PS-9	PS-15	ROC	REC	UC	OC	EC	No. of AFLP bands
No. 1	I	I	I	I	I	I	I	I	I	I	725
No. 2	II	II	II	II	II	II	II	II	II	II	422
No. 3	III	III	III	III	III	III	III	III	III	III	96
No. 4	I	–	–	–	–	–	–	–	–	–	6
No. 5	II	–	–	–	–	–	–	–	–	–	7
No. 6	III	–	–	–	–	–	–	–	–	–	7
No. 7	I	II	II	II	II	II	II	II	II	II	5
No. 8	I	III	III	III	III	III	III	III	III	III	4
No. 9	–	–	–	–	–	–	–	I	–	–	3
No. 10	–	–	–	–	–	–	–	II	–	–	5
No. 11	–	–	–	–	–	–	–	III	–	–	22
No. 12	–	–	–	–	–	–	–	–	I	–	10
No. 13	–	–	–	–	–	–	–	–	II	–	18
No. 14	–	–	–	–	–	–	–	–	III	–	10
No. 15	–	–	–	–	–	–	–	–	–	I	12
No. 16	–	–	–	–	–	–	–	–	–	II	3
No. 17	–	–	–	–	–	–	I	–	–	I	64
No. 18	–	–	–	–	–	–	II	–	–	II	19
No. 19	–	–	–	–	–	–	III	–	–	III	6
No. 20	–	–	–	–	–	–	II	–	–	I	16
No. 21	–	–	–	–	–	–	–	I	I	–	15
No. 22	–	–	–	–	–	–	–	II	II	–	4
No. 23	–	–	–	–	–	–	–	III	III	–	7
No. 24	II	II	II	II	II	II	II	–	II	II	5
No. 25	I	I	I	I	I	I	I	I	–	I	6
No. 26	II	II	II	II	II	II	II	II	–	II	13
No. 27	II	II	II	II	II	II	II	II	II	–	3
No. 28	II	II	II	II	II	II	II	–	–	II	21
No.29	III	III	III	III	III	III	–	III	III	–	3
Others											193

second group (Fig. 3), while UC and OC were clustered into a third group (Fig. 3). Interestingly, REC and ROC showed different methylation patterns, and fell into two different groups (Fig. 3).

Isolation, validation and sequencing of the three types of AFLP bands

Over 24 AFLP bands from different banding patterns were isolated from dried gels, and cloned into pBluescript KS vectors. For each AFLP band, eight clones were selected following standard PCR-based selection, and their inserts were found to be similar in size to the corresponding AFLP band. These eight clones were then subjected to selective amplification, using corresponding labeled *Eco*RI and nonlabeled *Hpa*II–*Msp*I primers. Clones containing inserts of the exact same size as that of their corresponding AFLP band were obtained (Fig. 4a). These clones were then deemed to be derived from the target AFLP band and were used for sequencing.

Further validation of cloned AFLP bands was performed using PCR assay and Southern hybridization. For each AFLP band, a pair of primers was designed, based on both ends of the sequenced insert and used to amplify the corresponding selective-amplification products in the AFLP analysis. If the primers were actually derived from the target AFLP band, then the PCR-banding patterns should be the same as those observed in the AFLP analysis. Furthermore, for a type I band, PCR products should be present under both *Msp*I and *Hpa*II in all tissues. For type II and type III bands, PCR products should appear under either *Msp*I (type II) or *Hpa*II (type III) in all tissues (Fig. 4b). For all observed tissue-specific AFLP bands, PCR-banding patterns should be also consistent with those obtained in the AFLP analysis.

Several cloned AFLP bands, including one type I, two type II, and two type III AFLP bands, were further labeled as probes for Southern hybridization to verify the fidelity of the previously described isolation and validation steps. In all cases, hybridization patterns were comparable to those observed in the AFLP analysis. Several high-molecular-weight hybridization bands appeared when using the labeled type II AFLP band P2-CG/AC-258 as a probe (Fig. 5a), indicating the presence of highly homologous sequences in the rose genome. In addition to the correct type III band P3-GT/AC-477 (477 bp) observed under *Hpa*II in all tissues, a small-sized band (~380 bp) was also observed under *Msp*I (Fig. 5b). This latter band corresponded to a fragment delimited by two 5′-CCGG-3′ sites present in this type III band.

Table 3 AFLP band type changes during shoot organogenesis and somatic embryogenesis in rose (*R. hybrida* L.)

AFLP band type[a]	GP→PS-9	PS-9→UC	UC→EC	EC→REC	UC→OC	OC→ROC	Total
I • → ^	25	7	34	21	12	41	140
II • → ^	17	34	29	8	30	33	151
III • → ^	14	16	44	9	31	27	141
I ^ → •	2	40	106	7	19	23	197
II ^ → •	3	18	59	10	27	46	163
III ^ → •	2	37	16	11	17	16	99
I → II	9	5	9	18	9	4	54
II → I	1	11	8	2	4	3	29
I → III	11	9	6	4	9	13	52
III → I	0	6	5	1	3	6	21

[a] *I* Type I AFLP band, *II* type II AFLP band, *III* type III AFLP band. • appearance, ^ disappearance, → change

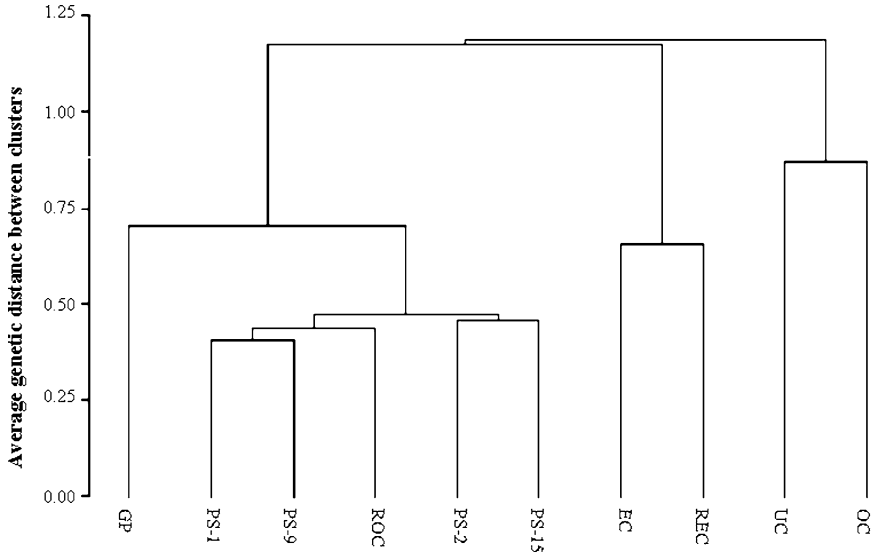

Fig. 3 Cluster analysis showing similarity of DNA-methylation profiles among various tissues of *R. hybrida* cv. Carefreee Beauty

A total of 19 AFLP bands belonging to six different banding patterns were sequenced and confirmed by a series of validation steps as described above (Table 4). Sequence analysis showed that an internal 5′-CCGG-3′ sequence was present in all five type III bands and in one out of six type II bands, but not in any of the seven type I bands. Meanwhile, a single type III band (P3-TG/AC-225) had two internal 5′-CCGG-3′ sequences (Table 4). These findings demonstrated some of the alterations observed in the three types of AFLP bands.

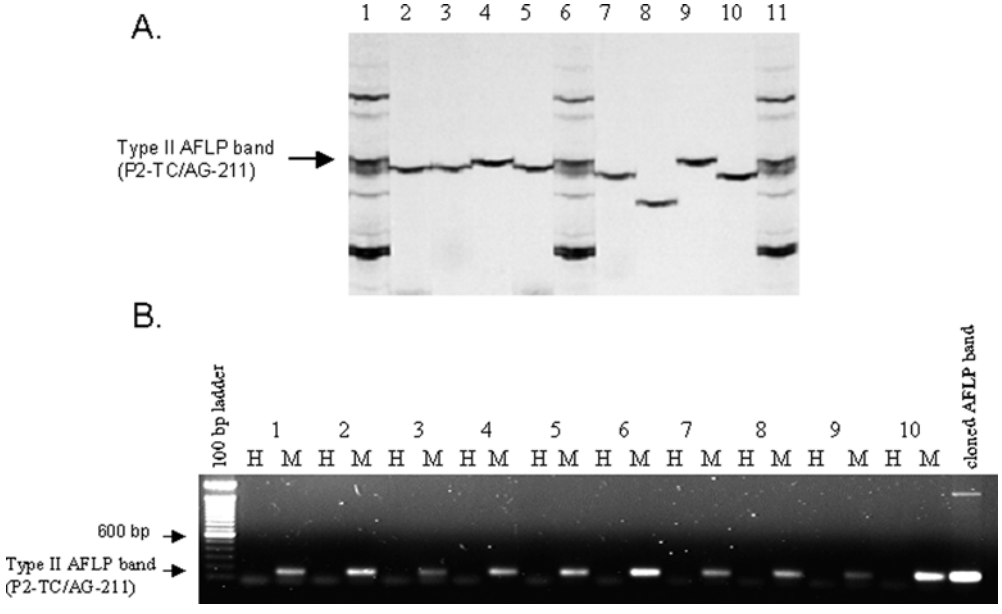

Fig. 4 **a** Identification of clones containing the authentic type II AFLP band. The type II AFLP band, P2-TC/AG-211, was excised from the dried gel and cloned into plasmid vector pBluescript-KS. The primer pair of 33P-labeled *Eco*RI+TC and *Hpa*II-*Msp*I+AG was used to amplify eight selected clones. The PCR products together with corresponding selective-amplification AFLP products were subjected to electrophoresis on a Longer-Ranger gel. The precise sizes of all cloned AFLP bands were identified and compared with their corresponding type II AFLP band. *Lanes 1*, *6*, and *11* are selective-amplification AFLP products of GP genomic DNA digested with *Eco*RI/*Msp*I. *Lanes 2–5* and *7–10* correspond to eight clones containing candidate type II AFLP bands. Out of eight clones, two clones (*lanes 4* and *9*) contain inserts of the exact same sizes as those of type II AFLP bands and are assumed to be the correct clones having type II bands. The *arrow* indicates a type II AFLP band. **b** Verification of a cloned AFLP band using PCR. A pair of PCR primers designed on a cloned type II AFLP band, P2-TC/AG-211, was used to amplify selective-amplification products in AFLP analysis. *Lanes H* and *M* correspond to two sets of restriction enzyme combinations: *Eco*RI/*Hpa*II and *Eco*RI/*Msp*I, respectively. *Lane 1* GP, *lane 2* PS-1, *lane 3* PS-2, *lane 4* PS-9, *lane 5* PS-15, *lane 6* ROC, *lane 7* REC, *lane 8* UC, *lane 9* OC, *lane 10* EC. The observed PCR-banding pattern was compatible with that in the AFLP analysis, indicating that the cloned AFLP band was an authentic type II AFLP band

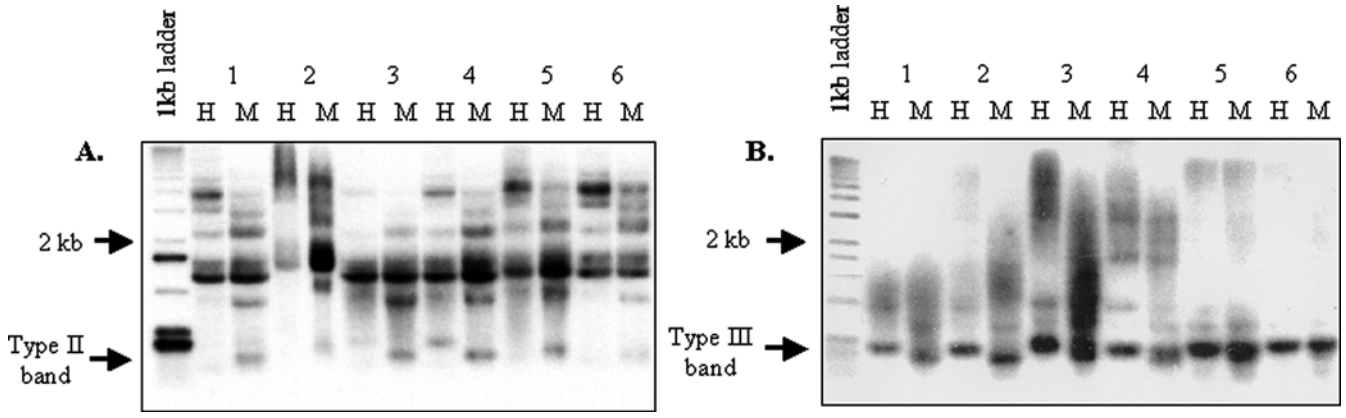

Fig. 5a, b Verification of DNA methylation using Southern hybridization. *Lanes H* and *M* correspond to two sets of restriction enzyme combinations: *Eco*RI/*Hpa*II and *Eco*RI/*Msp*I, respectively. *Lane 1* GP, *lane 2* PS-9, *lane 3* REC, *lane 4* UC, *lane 5* OC, *lane 6* EC. The probe was generated by PCR, using cloned AFLP bands as template DNA. **a** The hybridization pattern, using a labeled type II AFLP band P2-CG/AC-258. Except for that of PS-9, a hybridization band of 258 bp was present in each M lane; this band was comparable to a type II band in the corresponding AFLP analysis. Many hybridization bands of higher molecular weights were observed in each of the lanes, suggesting presence of highly homologous sequences in the rose genome. PS-9 showed differential hybridization patterns possibly due to partial digestion. **b** The hybridization, pattern using a labeled type III AFLP band, P3-GT/AC-477. A hybridization band of ~470 bp was present in each H lane; this band was comparable to a type III band in the corresponding AFLP analysis. A smaller hybridization band of ~380 bp was present in each M lane, except for that of OC. This band was consistent with the size delimited by two 5′-CCGG-3′ sequences of a type III AFLP band, and can be released with *MspI*. This confirmed that the internal methylated 5′-CCGG-3′ sequence was sensitive to *MspI*, but not to *HpaII*. The M lane of EC did not show a smaller hybridization band, which likely resulted from partial digestion

Blast search

Among all 19 AFLP bands that were sequenced, seven methylation-related bands were found to be tissue-specific and therefore were of interest, as they might be derived from genes that function differentially in various tissues. Five tissue-specific type I and two tissue-specific type II AFLP bands (Table 4) were subjected to Blast search to look for homologous sequences in the GenBank. Two bands, P17-CT/AG-260 and P22-GT/AG-237, were highly homologous to particular functional genes, DET1 (highest score of 124 bits and an E-value of 1e-28 for a tomato tDET1) and a Ca^{2+}-dependent, solute carrier-like protein (highest score of 94 bits and an E-value of 4e-19 for an *Arabidopsis thaliana* protein F5 k20.240), respectively (Fig. 6).

Table 4 Analysis of AFLP bands isolated from various banding patterns

Banding patterns	Names of AFLP bands	Primer combinations	Sizes (bp)	Internal 5′-CCGG-3′[a]
No. 1 (nonspecific type I)	P1-CT/AG-185	E-CT + HM-AG	185	−
	P1-GT/TC-218	E-GT + HM-TC	218	−
	P1-AC/AG-227	E-AC + HM-AG	227	−
No. 2 (nonspecific type II)	P2-TC/AG-211	E-TC + HM-AG	211	−
	P2-TC/AG-201	E-TC + HM-AG	201	+
	P2-TC/AG-341	E-TC + HM-AG	341	−
	P2-CG/AC-258	E-CG + HM-AC	258	−
No. 3 (nonspecific type III)	P3-TC/AG-286	E-TC + HM-AG	286	+
	P3-CG/TG-466	E-CG + HM-TG	466	+
	P3-TC/AG-285	E-TC + HM-AG	285	+
	P3-TG/AC-225	E-TG + HM-AC	225	++
	P3-GT/AC-477	E-GT + HM-AC	477	+
No. 17 (EC- and REC-specific type I)	P17-CT/AG-260	E-CT + HM-AG	260	−
	P17-AC/AC-214	E-AC + HM-AC	214	−
	P17-AC/AC-267	E-AC + HM-AC	267	−
	P17-CG/AC-339	E-CG + HM-AC	339	−
No. 20 (EC-specific type I)	P20-AC/AG-229	E-AC + HM-AG	229	−
No. 22 (UC- and OC-specific type II	P22-GT/AG-237	E-GT + HM-AG	237	−
	P22-TC/AG-239	E-TC + HM-AG	239	−

[a]− Absence of internal 5′-CCGG-3′ sequence, + presence of a single internal 5′-CCGG-3′ sequence, ++ presence of double internal 5′-CCGG-3′ sequences

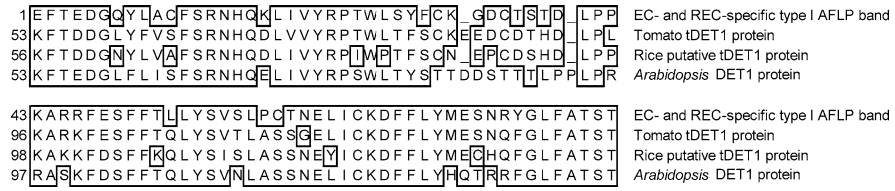

Fig. 6 Alignment of deduced amino acid sequences of an EC- and REC-specific type I AFLP band with homologous regions of DET1 proteins from tomato, rice, and *Arabidopsis*. Following Blast search, the deduced amino acid sequence of an EC- and REC-specific type I AFLP band was found to be highly homologous to DET1 proteins from tomato, rice, and *Arabidopsis*. This indicated that the EC- and REC-specific type I AFLP band was derived from the DET1 protein from rose. This suggested demethylation occurred during formation of the EC, and this was passed on to its regenerants. Identical and similar residues are *boxed*

Table 5 Alterations of AFLP bands caused by DNA-methylation modification at both inner and outer cytosines in *Msp*I/*Hpa*II sites adjacent to *Eco*RI sites

AFLP band type changes[a]	Methylation alteration in *Msp*I/*Hpa*II sites	Alterations of digested fragments	Frequency of amplification
I • → ^	5′-CCGG-3′ → 5′-mCCGG-3′	^ *Eco*RI-*Msp*I/ *Hpa*II (−)	
	5′-mCCGG-3′ → 5′-CCGG-3′	^ *Eco*RI-*Msp*I/*Hpa*II (+)	
	5′-mCmCGG-3′ → 5′-CmCGG-3′	^ *Eco*RI-*Msp*I/*Hpa*II (+)	
II • → ^	5′-CmCGG-3′ → 5′-mCmCGG-3′	^ *Eco*RI-*Msp*I (−)	
	5′-mCCGG-3′ → 5′-CCGG-3′	^ *Eco*RI-*Msp*I (+)	
	5′-mCmCGG-3′ → 5′-CmCGG-3′	^ *Eco*RI-*Msp*I (+)	
III • → ^	5′-CmCGG-3′ → 5′-CCGG-3′	^ *Eco*RI-*Hpa*II (+)	
	5′-CmCGG-3′ → 5′-mCmCGG-3′	^ *Eco*RI-*Hpa*II (+)	
	5′-mCCGG-3′ → 5′-CCGG-3′	^ *Eco*RI-*Hpa*II (++)	
	5′-mCmCGG-3′ → 5′-CmCGG-3′	^ *Eco*RI-*Hpa*II (++)	
I ^ → •	5′-mCCGG-3′ → 5′-CCGG-3′	• *Eco*RI-*Msp*I/*Hpa*II (−)	1
	5′-CCGG-3′ → 5′-mCCGG-3′	• *Eco*RI-*Msp*I/*Hpa*II (+)	1/4
	5′-CmCGG-3′ → 5′-mCmCGG-3′	• *Eco*RI-*Msp*I/*Hpa*II (+)	1/4
II ^ → •	5′-mCmCGG-3′ → 5′-CmCGG-3′	• *Eco*RI-*Msp*I (−)	1
	5′-CCGG-3′ → 5′-mCCGG-3′	• *Eco*RI-*Msp*I (+)	1/4
	5′-CmCGG-3′ → 5′-mCmCGG-3′	• *Eco*RI-*Msp*I (+)	1/4
III ^ → •	5′-CCGG-3′ → 5′-CmCGG-3′	• *Eco*RI-*Hpa*II (+)	1/4
	5′-mCmCGG-3′ → 5′-CmCGG-3′	• *Eco*RI-*Hpa*II (+)	1/4
	5′-CCGG-3′ → 5′-mCCGG-3′	• *Eco*RI-*Hpa*II (++)	1/16
	5′-CmCGG-3′ → 5′-mCmCGG-3′	• *Eco*RI-*Hpa*II (++)	1/16
I → II	5′-CCGG-3′ → 5′-CmCGG-3′	*Eco*RI-*Msp*I/ *Hpa*II (−) → *Eco*RI-*Msp*I (−)	1
II → I	5′-CmCGG-3′ → 5′-CCGG-3′	*Eco*RI-*Msp*I (−) → *Eco*RI-*Msp*I/*Hpa*II (−)	1
I → III	5′-CCGG-3′ → 5′-hmCCGG-3′	*Eco*RI-*Msp*I/ *Hpa*II (−) → *Eco*RI-*Hpa*II (−)	1
III → I	5′-hmCCGG-3′ → 5′-CCGG-3′	*Eco*RI-*Hpa*II (−) → *Eco*RI- *Msp*I/*Hpa*II (−)	1

[a] • Appearance, ^ disappearance, − absence of internal 5′-CCGG-3′ sequence, + presence of a single internal 5′-CCGG-3′ sequence, ++ presence of double internal 5′-CCGG-3′ sequences, *I* type I AFLP band, *II* type II AFLP band, *III* type III AFLP band, *M* methylation, *hm* hemi-methylation, → change

Discussion

Presence of three types of AFLP bands and their associated variations

In an AFLP analysis, only *Eco*RI–*Msp*I or *Eco*RI–*Hpa*II fragments are likely to be both amplified and visualized on an X-ray film. *Msp*I and *Hpa*II show no differences in cutting a nonmethylated 5′-CCGG-3′ sequence and therefore generate type I AFLP bands. However, differential sensitivity occurs when the inner cytosine in the 5′-CCGG-3′ sequence is methylated. In this case, only *Msp*I can cut the 5′-CmCGG-3′ sequence, and results in "standard" *Eco*RI–*Msp*I fragments without (an) internal 5′-CCGG-3′ sequence(s). *Hpa*II cannot cut the 5′-CmCGG-3′ sequence until it recognizes the next nonmethylated 5′-CCGG-3′ sequence, thus producing "long" *EcoR*I-*Hpa*II fragments with (an) internal 5′-CCGG-3′ sequence(s). It is almost certain that *Hpa*II will find the next nonmethylated 5′-CCGG-3′ sequence(s), as on

average, there are 16 *Msp*I/*Hpa*II-recognition sites (5′-CCGG-3′) within any two neighboring *Eco*RI-recognition sites (5′-GAATTC-3′), and most 5′-CCGG-3′ sequences are nonmethylated. Hypothetically, the number of "long" *Eco*RI–*Hpa*II fragments is almost the same as that of "standard" *Eco*RI–*Msp*I fragments. Due to the intrinsic limitation of the AFLP analysis that only short fragments (<1 kb) can be amplified and visualized on an X-ray film, "long" *Eco*RI–*Hpa*II fragments resulting in type III AFLP bands are less likely to be amplified compared to "standard" *Eco*RI–*Msp*I fragments producing type I and II AFLP bands. This is strongly supported by the results presented in this study. Firstly, all type III AFLP bands have either one or two internal 5′-CCGG-3′ sequence(s), whereas most type I and II AFLP bands do not contain (an) internal 5′-CCGG-3′ sequence(s). Secondly, the size of type III bands is on average larger than that of either type I or II bands. Thirdly, the number of type III bands is approximately one-fourth of that of type II bands. Similar ratios of type III to type II bands have also been observed in apple (one-fourth, Xu et al. 2000) and in rice (one-seventh, Xiong et al. 1999), respectively. It can then be concluded that the presence of an inner 5mC in the 5′-CCGG-3′ sequence is mainly responsible for the observed type II and type III AFLP bands. Xiong et al. (1999) have attributed occurrence of type III bands solely due to the hemimethylation of the outer cytosine. This is in contrast to the results obtained in this study. If hemimethylation of the outer cytosine is the only reason causing the occurrence of type III bands, most type III AFLP bands must not contain (an) internal 5′-CCGG-3′ sequence(s), and the average sizes of type II and III AFLP bands must be similar. The hemimethylation of the outer cytosine will result in an exchange between type I and type III bands, and such an exchange is observed in this study, but only at very low levels (Tables 3, 5).

Analysis of tissue-specific AFLP bands reveals a total of ten different alterations among the three types of AFLP bands, including the appearance and disappearance of type I, II, and III AFLP bands and exchanges between either type I and type II or between type I and type III bands (Tables 2, 3). The appearance and disappearance of type I and type II AFLP bands can only be achieved by modifying the outer cytosine in the 5′-CCGG-3′ sequence (Table 5). Methylation of the outer cytosine in either 5′-CCGG-3′ or 5′-CmCGG-3′ sequence will block the functioning of both *Msp*I and *Hpa*II, resulting in the disappearance of type I, II, and III AFLP bands. Meanwhile, both *Msp*I and *Hpa*II may recognize the next 5′-CCGG-3′ sequence and generate new *Eco*RI–*Msp*I and *Eco*RI–*Hpa*II fragments. Both new *Eco*RI–*Msp*I and *Eco*RI–*Hpa*II fragments will be identical if the next 5′-CCGG-3′ sequence is nonmethylated. Whereas, the *Eco*RI–*Hpa*II fragment will be longer than that of an *Eco*RI–*Msp*I fragment if the inner cytosine of the next 5′-CCGG-3′ sequence is methylated. All newly generated fragments carry (an) internal 5′-CCGG-3′ sequence(s), and therefore are less likely (only one-fourth probability, as estimated above) to be amplified and visualized on an X-ray film (Table 5). In contrast, demethylation of the outer cytosine will generate shorter *Eco*RI–*Msp*I or *Eco*RI–*Hpa*II fragments. When the 5′-mCCGG-3′ changes to 5′-CCGG-3′, both *Eco*RI–*Msp*I and *Eco*RI–*Hpa*II fragments will be shortened and result in the appearance of type I AFLP bands. When a 5′-mCmCGG-3′ is altered to a 5′-CmCGG-3′, a "standard" *Eco*RI–*Msp*I fragment and a "long" *Eco*RI–*Hpa*II fragment will be generated, thus yielding new type II and III AFLP bands, respectively (Table 5).

Demethylation of an inner cytosine in a 5′-CmCGG-3′ sequence leads to the removal of type III bands as well as substitution of type I for type II bands. In contrast, methylation of an inner cytosine in a 5′-CCGG-3′ sequence results in the generation of type III bands as well as substitution of type II for type I bands (Table 5). Hemimethylation of the outer cytosine in a 5′-CCGG-3′ sequence allows for functioning of *Hpa*II, but not of *Msp*I, thus replacing type I with type III AFLP bands. In contrast, removal of hemimethylation from the outer cytosine in a 5′-hmCCGG-3′ sequence activates both *Hpa*II and *Msp*I, thus altering type III into type I AFLP bands (Table 5). Previously, McClelland et al. (1994) have reported that *Hpa*II is inactive if one or both cytosines are fully methylated (both strands are methylated), but it cleaves as hemimethylated sequence (only one strand is methylated), whereas *Msp*I cleaves C5mCGG, but not 5mCCGG. This further supports the findings observed in this study.

Overall, disappearance of type I and II AFLP bands is mainly due to methylation of the outer cytosine of the 5′-CCGG-3′ and 5′-CmCGG-3′ sequences, respectively, while appearance of type I and II AFLP bands is largely due to demethylation of the outer cytosine of the 5′-mCCGG-3′ and 5′-mCmCGG-3′ sequences, respectively. However, appearance and disappearance of type III AFLP bands involve both inner and outer cytosines. Methylation alteration of the inner cytosine is responsible for exchanges between type I and type II bands. Sequence analysis has confirmed our conclusion that all type I, three out of four type II, and all newly generated type I and II AFLP bands do not contain any internal 5′-CCGG-3′ sequence(s) (Table 4). A single type II band, P2-TC/AG-201, contains an internal 5′-CCGG-3′ sequence, and is most likely caused by an outer 5mC (Table 3).

Estimation of frequencies for both inner and outer methylcytosines in 5′-CCGG-3′ sequences

For a nonmethylated 5′-CCGG-3′ sequence, both *Eco*RI–*Msp*I and *Eco*RI–*Hpa*II fragments are equally amplified and displayed as type I AFLP bands, while for the 5′-CmCGG-3′ sequence with an inner methylcytosine, only an *Eco*RI–*Msp*I fragment is normally amplified and displayed as a type II AFLP band. Therefore, the frequency of an inner methylcytosine in the 5′-CCGG-3′ sequence can be easily and accurately estimated by dividing the number of type II bands by the total number

of type I+II bands. In this study, ~40% of inner cytosines in the 5′-CCGG-3′ sequence are estimated to be methylated in *R. hybrida* cv. Carefree Beauty. Approximately, 21% and 17% of inner methylated cytosines have been estimated in apple (Li et al. 2002a) and rice (Xiong et al. 1999), respectively. The frequency of external methylated cytosines in the 5′-CCGG-3′ sequence can also be roughly estimated in this study. A total of 16 type I and II AFLP bands have been sequenced, but only a single type II band, P2-TC/AG-201, contains an internal 5′-CCGG-3′ sequence. The 5′-mCCGG-3′ sequences with outer methylated cytosines will result in the recovery of "long" *Eco*RI–*Msp*I fragments containing an internal 5′-CCGG-3′ sequence. On an average, only one-fourth of such "long" fragments are amplified and displayed on an X-ray film based on the above analysis. Therefore, the frequency of outer 5mC in 5′-CCGG-3′ sequences can be estimated using the following formula: $(4\times a)/([4\times a]+b)$; whereby, a corresponds to the number of type I and II bands with an internal 5′-CCGG-3′ sequence, and b corresponds to the number of type I and II bands lacking an internal 5′-CCGG-3′ sequence. In this study, 20% of outer cytosines are estimated to be methylated in the 5′-CCGG-3′ sequence. However, as the sample size is rather small, this estimation may be biased. Gruenbaum et al. (1981) have estimated that ~50% of 5′-CCGG-3′ sites are modified along the outer cytosines in wheat embryos and tobacco leaves, which are much higher than those estimated in the rose genome.

Relationships of different alterations among the three types of AFLP bands

The relationships among ten different variations observed in the three types of AFLP bands can be inferred from analyzing the frequencies of methylated outer and inner cytosines and methylation events underlying variations in types of AFLP bands. As methylation of the outer cytosine of the 5′-CCGG-3′ and 5′-CmCGG-3′ sequences is mainly responsible for the disappearance of type I and II AFLP bands, respectively (Table 5), and the frequency of 5′-CmCGG-3′ sequences is estimated to be 40% in the rose genome, the number of disappearing type II bands must be two-thirds of those type I disappearing bands. Likewise, the numbers of appearing type II AFLP bands must be two-thirds of those appearing type I AFLP bands. These estimations can be roughly confirmed in this study (Table 3). Four different methylation events have resulted in the appearance of new type III AFLP bands. The first event also caused substitution of type II for type I bands; while, the remaining three events caused the appearance of type II bands (Table 5). Since a "long" *Eco*RI-*Hpa*II fragment containing (an) internal 5′-CCGG-3′ sequence(s) has only a one-fourth probability of being amplified and displayed on a film, the number of newly generated type III AFLP bands is therefore only one-fourth of those substituted type II for type I combined with those newly generated type II bands. Likewise, the number of disappearing type III AFLP bands is only one-fourth of those substituted type I for type II and disappearing type II. In this study, the newly generated type III AFLP bands are close to this estimation; however, the number of disappearing type III AFLP bands is much higher than the estimated value (Table 3). It is surprising that methylation alterations of outer cytosines in the rose genome are far more frequent than those of inner cytosines, as the number of disappearing and appearing type I and II AFLP bands are much higher than those exchanges between type I and II AFLP bands.

Methylation alterations during somatic embryogenesis and shoot organogenesis

By analyzing changes in the three types of AFLP bands observed during somatic embryogenesis and shoot organogenesis, vivid features of alterations in DNA methylation during cellular reprogramming events can be discerned. During induction of UC from PS-9, high frequency of alterations in methylation patterns have been observed, including methylation and demethylation of both inner and outer cytosines in (a) 5′-CCGG-3′ sequence (s). The most striking feature is the generation of 37 new type III bands. As only one-fourth of the "long" *Eco*RI–*Hap*II fragments containing (an) internal 5′-CCGG-3′ sequence(s) are detected on a film, then these newly generated type III bands suggest the following: there are approximately four times as many methylations of inner cytosines in 5′-CCGG-3′ sequences and similarly as many demethylations of outer cytosines in 5′-$_{m}$C$_{m}$CGG-3′ sequences occurring during the induction of UC of rose.

Methylation alterations during somatic embryogenesis in rose are characterized by extensive demethylation of outer cytosines in 5′–$_{m}$CCGG-3′ sequences, and these are passed along to their REC. EC has the highest number of type I bands compared to all other rose tissues analyzed (Table 1). A total of 106 new type I and 59 new type II AFLP bands are generated during induction of EC from UC, and this is higher than in any of the other observed cellular differentiation processes (Table 3). EC and REC in rose share many modified AFLP bands (Table 2), and these are clustered into the same group (Fig. 3). The most significant difference between EC and REC is that 16 type I bands in EC have been exchanged into type II bands in REC (Table 2, no. 20). This indicates that a number of inner cytosines are methylated during the development of REC from EC. This is in contrast to methylation alterations observed during organogenesis, whereby various alterations in methylation have been noted during the development of OC from UC and subsequently during development of ROC from OC. Almost all modified cytosines during organogenesis in rose are recovered in ROC, thus resulting in almost identical methylation patterns in ROC and in PS-1 to PS-9 (Table 2; Fig. 3).

Methylation patterns and morphogenesis

It is important to correlate alterations in DNA methylation with observed morphogenic changes. Diaz-Sala et al. (1995) have suggested that in addition to genetic controls, epigenetic controls due to DNA methylations are likely to be involved in the acquisition of morphogenic competence of greenhouse-grown leaf tissues following sequential in vitro subcultures, i.e., subsequent passages. Munksgaard et al. (1995) and Chakrabaty et al. (2003) have reported that remethylation occurs in bipolar plants when they develop from EC. In many plant species, particular groups of genes are temporally and spatially expressed during embryogenesis (Goldberg et al. 1989), whereas original embryogenic cells or germline cells in animals contain either unmethylated or hypomethylated DNA (Chaillet et al. 1991; Monk et al. 1987). DNA hypomethylation resulting from treatment of somatic cells with ethylene may lead to acquisition of the embryogenic potential (Herman 1991; Okkels 1988). Munksgaard et al. (1995) have proposed that levels of S-adenosylmethionine and S-adenosylhomocysteine may initially affect the level of DNA methylation, which in turn may control somatic embryogenesis and result in differential changes in gene activation. Kaeppler and Phillips (1993b) have reported that DNA methylation involved in certain DNA fragments decreases in maize regenerants, and these changes in DNA methylation are stably inherited after two generations of self-pollination.

In the rose genome, DNA-methylation alterations during reprogramming of somatic tissues are associated with cellular differentiation pathways. Methylation patterns during somatic embryogenesis appear to be quite different from those during shoot organogenesis as is clearly demonstrated in the cluster analysis. It may be conceivable that DNA-methylation patterns in EC differ from those in OC due to their apparent differences in cellular differentiation pathways. However, it is more difficult to explain differences in DNA-methylation patterns between REC and ROC, as they are less likely to exhibit phenotypic differences. Thus, one proposed explanation for this observed phenomenon is that all altered DNA methylations, especially demethylation of outer cytosines, are only related to embryogenic ability. To further elucidate this hypothesis, two rose REC individuals, REC-41 and REC-43, have been subjected to somatic embryogenesis. The embryogenic abilities of REC-41 and REC-43 are much higher than those of other in vitro-grown shoots (data not shown). This supports the hypothesis that modified cytosines may be essential for the acquisition of embryogenic potential in somatic cells, and these are then passed on to subsequent regenerants. As a consequence, the embryogenic ability is greatly enhanced via somatic embryogenesis. Delbreil and Jullien (1994) have reported that high regeneration ability can be acquired following in vitro selection of habituated totipotent cells during somatic embryogenesis. Although we are proposing that this is due to epigenetics caused by methylation alterations, it is also possible that this is also caused by some DNA (or gene) mutations. Brown (1989) has suggested that plant cells undergo stress during tissue culture leading to significant changes in methylation, and by subsequent deamination and poor mismatch repairs, this leads to DNA mutations or alterations.

The clustering of the methylation patterns of ROC with PS is to be expected as ROC develops into organized shoots (Fig. 3). Similarly the clustering of methylation patterns of EC and REC is also to be expected; however, the clustering of UC with OC suggests that the methylation patterns of these two types of tissues are more divergent than those for all other groups of morphogenetic tissues.

The deduced amino acid sequence of P17-CT/AG-260 is likely derived from the DET1 protein in *R. hybrida* cv. Carefree Beauty, as it shows high sequence homology with the DET1 protein of tomato, rice, and *A. thaliana* (Fig. 6). The function of this protein remains unclear. It has been reported that this protein influences the expression of large numbers of genes by upregulating transcription, perhaps through reorganization of repressive regions of the chromatin in the dark (Chory et al. 1996; Mustilli and Bowler 1997; Mustilli et al. 1999). The deduced amino acid sequence of P22-GT/AG-237 is likely to be a part of a Ca^{2+}-dependent, solute carrier-like protein (Fig. 6).

These observed differences in DNA methylation in rose tissues may be attributed to presence of PGRs in the culture medium and/or in vitro growth conditions (Kaeppler and Phillips 1993a, b; Li et al. 2002a; Pavlica et al. 1991). The chemical 2,4-D is known to induce chromosome aberrations in plants, both in vivo and in vitro, and also exerts selection pressure favoring changes in ploidy levels (Ronchi et al. 1976). Moreover, recovery or elimination of repetitive DNA sequences from a genome may lead to either higher or lower DNA content per nucleus, thus resulting in marked changes in genome organization (Arnholdt-Schmitt 1995). Finally, differences in DNA-methylation patterns from cell to cell within rose tissues may also result in additional changes in DNA polymorphisms.

Acknowledgements This work was supported by funding received from the Fred C. Gloeckner Foundation.

References

Arnholdt-Schmitt B (1995) Physiological aspects of genome variability in tissue culture. I. Growth phase-dependent quantitative variability of repetitive BstN I fragments of primary cultures of *Daucus carota* L. Theor Appl Genet 91:816–823

Bartee L, Malagnac F, Bender J (2001) *Arabidopsis cmt3* chromomethylase mutations block non-CG methylation and silencing of an endogenous gene. Genes Dev 15:1753–1758

Brown PTH (1989) DNA methylation in plants and its role in tissue culture. Genome 31:717–729

Cervera M-T, Ruiz-García L, Martínez-Zapater JM (2002) Analysis of DNA methylation in *Arabidopsis thaliana* based on methylation-sensitive AFLP markers. Mol Gen Genomics 268:543–552

Chaillet JR, Vogt TV, Beier DR, Leder P (1991) Parental-specific methylation of an imprinted transgene is established during gametogenesis and progressively changes during embryogenesis. Cell 66:77–83

Chakrabaty D, Yu KW, Paek KY (2003) Detection of DNA methylation changes during somatic embryogenesis of Siberian ginseng (*Eleuterococcus senticosus*). Plant Sci 165:61–68

Chory J, Chatterjee M, Cook RK, Elich T, Fankhauser C, Li J, Najpal P, Neff M, Pepper A, Poole D, Reed J, Vitart V (1996) From seed germination to flowering, light controls plant development via the pigment phytochrome. Proc Natl Acad Sci USA 93:12066–12071

Delbreil B, Jullien M (1994) Evidence for in vitro induced mutation which improves somatic embryogenesis in *Asparagus officinalis* L. Plant Cell Rep 13:372–376

Diaz-Sala C, Rey M, Boronat A, Besford R, Rodriguez R (1995) Variation in the DNA methylation and polypeptide patterns of adult hazel (*Corylus avellana* L.) associated with sequential in vitro subcultures. Plant Cell Rep 15:218–221

Duncan RP (1997) Tissue culture-induced variation and crop improvement. Adv Agron 58:201–240

Ferguson-Smith AC, Surani MA (2001) Imprinting and the epigenetic asymmetry between parental genomes. Science 293:1086–1089

Finnegan EJ (2001) Is plant gene expression regulated globally? Trends Genet 17:361–365

Goldberg RB, Barker SJ, Perez-Grau L (1989) Regulation of gene expression during plant embryogenesis. Cell 56:149–160

Gruenbaum Y, Naveh-Many T, Cedar H, Razin A (1981) Sequence specificity of methylation in higher plant DNA. Nature 292:860–862

Hecht V, Vielle-Calzada J-P, Hartog MV, Schmidt EDL, Boutilier K, Grossniklaus U, de Vries SC (2001) The *Arabidopsis* somatic embryogenesis receptor dinase 1 gene is expression in developing ovules and embryos and enhances embryogenic competence in culture. Plant Physiol 127:803–816

Herman EB (1991) Recent advances in plant tissue culture, regeneration, micro-propagation and media 1988–1991. Ethylene, DNA methylation and regeneration. Agritech. Consultant, Shrub Oak, pp 6–10

Kaeppler SM, Phillips RL (1993a) DNA methylation and tissue culture-induced variation in plants. In Vitro Cell Dev Biol 29:125–130

Kaeppler SM, Phillips RL (1993b) Tissue culture-induced DNA methylation variation in maize. Proc Natl Acad Sci USA 90:8773–8776

Kaeppler SM, Kaeppler HF, Rhee Y (2000) Epigenetic aspects of somaclonal variation in plants. Plant Mol Biol 43:179–188

Knox MR, Ellis THN (2001) Stability and inheritance of methylation states at *Pst*I sites in *Pisum*. Mol Genet Gen 265:497–507

Li X, Xu M, Korban SS (2002a) DNA methylation profiles differ between field- and in vitro-grown leaves of apples. J Plant Physiol 159:1229–1234

Li X, Krasnyanski S, Korban SS (2002b) Somatic embryogenesis, secondary somatic embryogenesis, and shoot organogenesis in *Rosa*. Plant Physiol 159:313–319

LoSchiavo F, Pitto L, Giuliano G, Torti G, Nuti-Ronchi V, Marazziti D, Vergara R, Orselli S, Terzi M (1989) DNA methylation of embryogenic carrot cell cultures and its variations as caused by mutation, differentiation, hormones and hypomethylating drugs. Theor Appl Genet 77:325–331

Matthes M, Singh R, Cheah SC, Karp A (2001) Variation in oil palm (*Elaeis guineensis* Jacq.) tissue culture-derived regenerants revealed by AFLPs with methylation-sensitive enzymes. Theor Appl Genet 102:971–979

McClelland M, Nelson M, Raschke E (1994) Effect of site-specific modification on restriction endonucleases and DNA modification methyltransferases. Nucleic Acids Res 22:3640–3659

Monk M, Boulebelik M, Lehnert S (1987) Temporal and regional changes in DNA methylation in the embryogenic, extraembryonic and germ cell lineages during mouse embryo development. Development 99:371–382

Mumm RH, Dudley JW (1995) A PC SAS computer program to generate a dissimilarity matrix for cluster analysis. Crop Sci 35:925–927

Munksgaard D, Mattsson O, Okkels FT (1995) Somatic embryo development in carrot is associated with an increase in levels of S-adenosylmethionine, S-adenosylhomocysteine and DNA methylation. Plant Physiol 93:5–10

Mustilli AC, Bowler C (1997) Tuning in to the signals controlling photoregulated gene expression in plants. EMBO J 16:5801–5806

Mustilli AC, Fenzi F, Ciliento R, Alfano F, Bowler C (1999) Phenotype of the tomato *high pigment-2* mutant is caused by a mutation in the tomato homolog of *DEETIOLATED1*. Plant Cell 11:145–157

Ng HH, Bird AP (1999) DNA methylation and chromatin modification. Curr Opin Genet Dev 9:158–163

Okkels FT (1988) A theory explaining formation of somatic embryogenic cells by auxin induced inhibition of DNA methylation. Plant Physiol 73:11

Pavlica M, Nagy B, Papes D (1991) 2,4-D causes chromosome and chromatin abnormalities in plant cells and mutation in cultured mammalian cells. Mutat Res 263:77–82

Reyna-López GE, Simpson J, Ruiz-Herrera J (1997) Differences in DNA methylation patterns are detectable during the dimorphic transition of fungi by amplification of restriction polymorphisms. Mol Gen Genet 253:703–710

Ronchi VN, Martini G, Buiatti M (1976) Genotype-hormone interaction in the induction of chromosome aberrations: effect of 2,4-dichlorophenoxyacetic acid (2,4-D) and kinetin on tissues from *Nicotiana* spp. Mutat Res 36:67–72

Rossi V, Motto M, Pellegrin L (1997) Analysis of the methylation pattern of the maize Opaque-2 (O2) promoter and in vitro binding studies indicate that the O2 B-Zip protein and other endosperm factors can bind to methylated target sequences. J Biol Chem 272:13758–13765

Sambrook J, Fritsch EF, Maniatis T (1989) Molecular cloning: a laboratory mannual, 2nd edn. Cold Spring Harbor Laboratory Press, Cold Spring Harbor, N.Y.

Stam M, Mol JNM, Kooter JM (1997) The silence of genes in transgenic plants. Ann Bot 79:3–12

Stancheva I, Maarri O, Walter J, Niveleau A, Meehan R (2002) DNA methylation at promoter regions regulates the timing of gene activation in *Xenopus laevis* embryos. Dev Biol 243:155–165

Sung ZR, Fienberg A, Chorneau R, Borkird C, Furner I, Smith J, Terzi M, Loschiavo F, Giuliano G, Pitto L, Nuti-Ronchi V (1984) Developmental biology of embryogenesis from carrot culture. Plant Mol Biol Rep 2: 216–218

The Arabidopsis Genome Initiative (2000) Analysis of the genome sequence of the flowering plant *Arabidopsis thaliana*. Nature 408:796–813

Wolffe AP, Matzke MA (1999) Epigenetics: regulation through repression. Science 286:481–486

Xiong LZ, Xu CG, Saghai-Maroof MA (1999) Patterns of cytosine methylation in an elite rice hybrid and its parental lines, detected by a methylation-sensitive amplification polymorphism technique. Mol Gen Genet 261:439–446

Xu ML, Li XQ, Korban SS (2000) AFLP-based detection of DNA methylation. Plant Mol Biol Rep 18:361–368

Xu ML, Ernesto H, Korban SS (2001) Development of sequence-characterized amplified regions (SCAR) from amplified fragment length polymorphism (AFLP) markers tightly linked to the *Vf* gene in apple. Genome 44:63–70